

Hydrometeorological features of Koryto glacier in the Kronotsky Peninsula, Kamchatka, Russia

Yuji KODAMA¹, Takane MATSUMOTO¹, Gleb E. GLAZIRIN², Yaroslav D. MURAVYEV³, Takayuki SHIRAIWA¹ and Satoru YAMAGUCHI¹

¹ Institute of Low Temperature Science, Hokkaido University, Sapporo 060 Japan

² Central Asian Research Hydrometeorological Institute, 700052 Tashkent, Uzbekistan

³ Institute of Volcanology, Russian Academy of Sciences, Piip Boulevard 9, Petropavlovsk-Kamchatky, Russia

(Received April 7, 1997 ; Revised manuscript received April 28, 1997)

Abstract

Meteorological observations were carried out at ablation and accumulation stations of the Koryto glacier, Kamchatka, in order to understand the characteristics of melting heat balance components. The results of the heat balance calculation showed that the largest heat source for the glacier ablation is the net radiation, which is, as an average, about 45 % of the total heat used for the melting. The second largest is the sensible heat flux and the third is the latent heat flux, which are about 30 % and 25 % of the snowmelt heat, respectively. When the large daily snowmelt occurs, the largest heat source for the snowmelt is sometimes not the net radiation but the turbulent heat fluxes.

Hydrological observations were carried out at two runoff streams from Koryto glacier. In Stream A, which had more than 5 times larger discharge than that of Stream B, water level, water temperature and specific electric conductivity were recorded. The discharge of Stream A increased gradually from 5.5 m³/s to 7.5 m³/s. The daily maximum discharge occurred about 3 hours later than the solar noon and the time lag was increased when the discharge became larger. The relationship between the specific electric conductivity and the discharge rate showed that the dilution of in-glacier constituent and/or stream bed material was progressing. Those hydrological results indicate that the ablation is in its beginning stage.

1. Introduction

It has long been waited for Japanese scientists to do research on glaciers in Kamchatka. The Kamchatka peninsula is located just north of Hokkaido. In Hokkaido, there are no glaciers existed now, but perennial snow patches exist and many Japanese glaciologist have studied on them. It is common for Japanese snow patch researchers to dream about that perennial snow patches in Hokkaido could have been a glacier in the last glacier age, or it would become a glacier in the coming glacier age. They think the past and/or future glaciers in Hokkaido would be like the glaciers in Kamchatka. However, the Kamchatka was closed to foreigners for a long time, and just recently opened. In the summer of 1996, a group of

the Institute of Low Temperature Science, Japan and an Uzbekistan glaciologist with a great help from Institute of Volcanology, could carry out a meteorological, hydrological and glaciological research in the summer of 1996 funded by International Science Program of the Ministry of Education, Science, Sport and Culture.

Our main goal for the research is to understand the response of the glaciers to environmental change, such as global warming. The Kamchatka peninsula is a part of the circum Okhotsk region, and this area is very interesting because the Okhotsk Sea area is surrounded by Siberian high and Aleutian low pressure systems, and it is the ocean where southernmost sea ice can be formed. The climate in Kamchatka must be immensely affected by the activity of

Aleutian lows and Siberian highs, as well as the sea ice extent in Okhotsk Sea.

Glaciers' mass balance is also influenced by the climatic conditions and the filtered climatic signals could be kept in the glacier. For example, winter precipitation and summer melting together would be found in the mass balance amount, which can be observed in the stratigraphy, and atmospheric constituents in the chemical constituents of snow/ice. However, in order to interpret these signals into past climatic conditions, we must know how they are taking in or how they are changed after. Therefore, it is very important to know the basic processes of the accumulation and ablation of the glacier responding to the environmental conditions.

In the summer of 1996, we obtained some hydrological and meteorological data in order to discuss on heat exchange between the atmosphere and the Koryto glacier, Kronotsky peninsula and its discharge to a stream at the terminus of the glacier. In this paper, the observed hydrometeorological data are shown and the glacier-melt heat balance and its discharge are discussed.

2. Site description

The observation site is described in the chapter 2 of "Regional settings" of Shiraiwa *et al.* (1997).

3. Observation

In order to understand the basic processes for the mass balance of the Koryto Glacier, hydrometeorological observation were carried out from July 9 to July 19, 1996. Especially, the snowmelt processes and their discharge to river were paid attention. For this purpose, three stations are set up. One is a meteorological station at accumulation area, second one is the same one at ablation area and third one hydrological station at the river near the terminus of the glacier. The measured elements are summarized in Table 1.

The meteorological components measured at the ablation area (545 m a.s.l., Fig. 1) are : net radiation (height from the ground : 1 m), global radiation (1 m), air temperature (1.5 m), humidity (1.5 m), wind speed (3.5 m), wind direction (1.5 m), snow surface temperature (0.3 m) and precipitation (0.5 m) (Table 1). Due to a logging error, net radiation and wind speed were

Table 1. Observed meteorological and hydrological elements and period.

Meteorological Observations	
Ablation station	Period
Net Radiation	96/7/13 – 96/7/19
Global Radiation	96/7/9 – 96/7/19
Air Temperature	96/7/9 – 96/7/19
Humidity	96/7/9 – 96/7/19
Wind Speed	96/7/13 – 96/7/19
Wind Direction	96/7/9 – 96/7/19
Snow Surface Temperature	96/7/9 – 96/7/19
Atmospheric Pressure	96/7/9 – 96/7/19
Precipitation	96/7/9 – 96/7/19
Accumulation station	
Net Radiation	96/7/14 – 96/7/17
Global Radiation	96/7/9 – 96/7/17
Air Temperature	96/7/9 – 96/7/17
Humidity	96/7/9 – 96/7/17
Wind Speed	96/7/13 – 96/7/17
Wind Direction	96/7/9 – 96/7/17
Snow Surface Temperature	96/7/9 – 96/7/17
Atmospheric Pressure	96/7/9 – 96/7/17
Precipitation	96/7/9 – 96/7/17
Hydrological observations	
Water Level	96/7/8 – 96/7/19
Water Temperature	96/7/8 – 96/7/19
Electric Conductivity	96/7/8 – 96/7/19

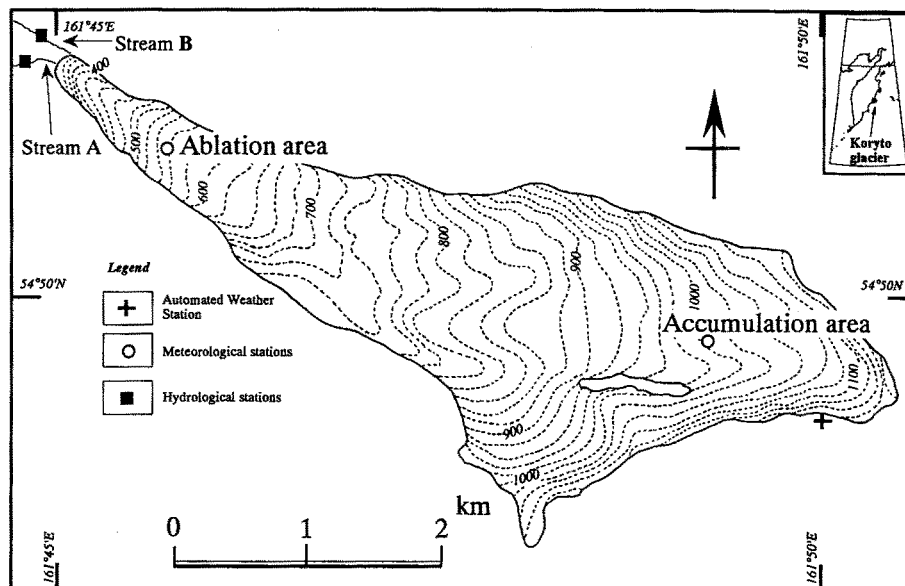


Fig. 1 Contour map of Koryto Glacier. Locations of observation points are plotted by symbols.

not recorded until July 13, whereas the other elements were measured from July 9 to July 19.

The measurements at the accumulation area (1005 m a.s.l., Fig. 1) were the same as the one at ablation area. Since the setting were moved to a ridge of the glacier watershed for the year round operation, the data were taken until July 17.

Hydrological observations were carried out at two streams of Koryto Glacier. Stream A (Fig. 1), which had greater discharge than Stream B, flows from the center of the terminus, and Stream B flows on the right side of the valley. The hydrological data were mainly collected at the Stream A (250 m a.s.l.) about 100 m downstream from the terminus of the glacier. When we started the measurements, the most of the river were covered by seasonal snow, and we could not choose the best place for the flow rate measurement but the snow-free area.

4. Results

4.1 Observed meteorological elements

The obtained meteorological elements are shown in Fig. 2. The solid line shows the elements obtained at the ablation station and the broken line at the accumulation station except precipitation, which is indicated in the figure.

4.1.1 Air temperature and vapor pressure

Air temperature showed above 0°C in the whole observation period. The daily range of the air temperature was from 3 °C to 10 °C. As the result of this and the positive net radiation, the snow surface temperature was 0°C all the time (not shown. The negative net radiation some times did not cool the snow surface enough to reach below 0°C.). The diurnal variation of air temperature was not clear for the both station. It might be due to the melting snow surface, which temperature is always kept to 0°C and acts as a heat sink consuming latent heat for melting. The melting heat balance of the snow surface will be discussed later.

The difference in air temperature for the two stations is interesting. The difference is not consistent even though the elevation difference is 460 m. If the air parcel at the accumulation station comes down adiabatically to the ablation station, the air temperature at the accumulation station would be 2.8 to 4.6 °C lower than that at the ablation station, assuming the adiabatic lapse rate of 0.6 to 1.0 °C/100 m. It is not clear that the air parcel at the ablation station comes from the accumulation station, only by the wind direction of the two stations, even though the wind at the ablation station is mainly from the upstream of the glacier. From the evening of July 12 to the noon of July 14 and partly on July 15 and July 16, air tempera-

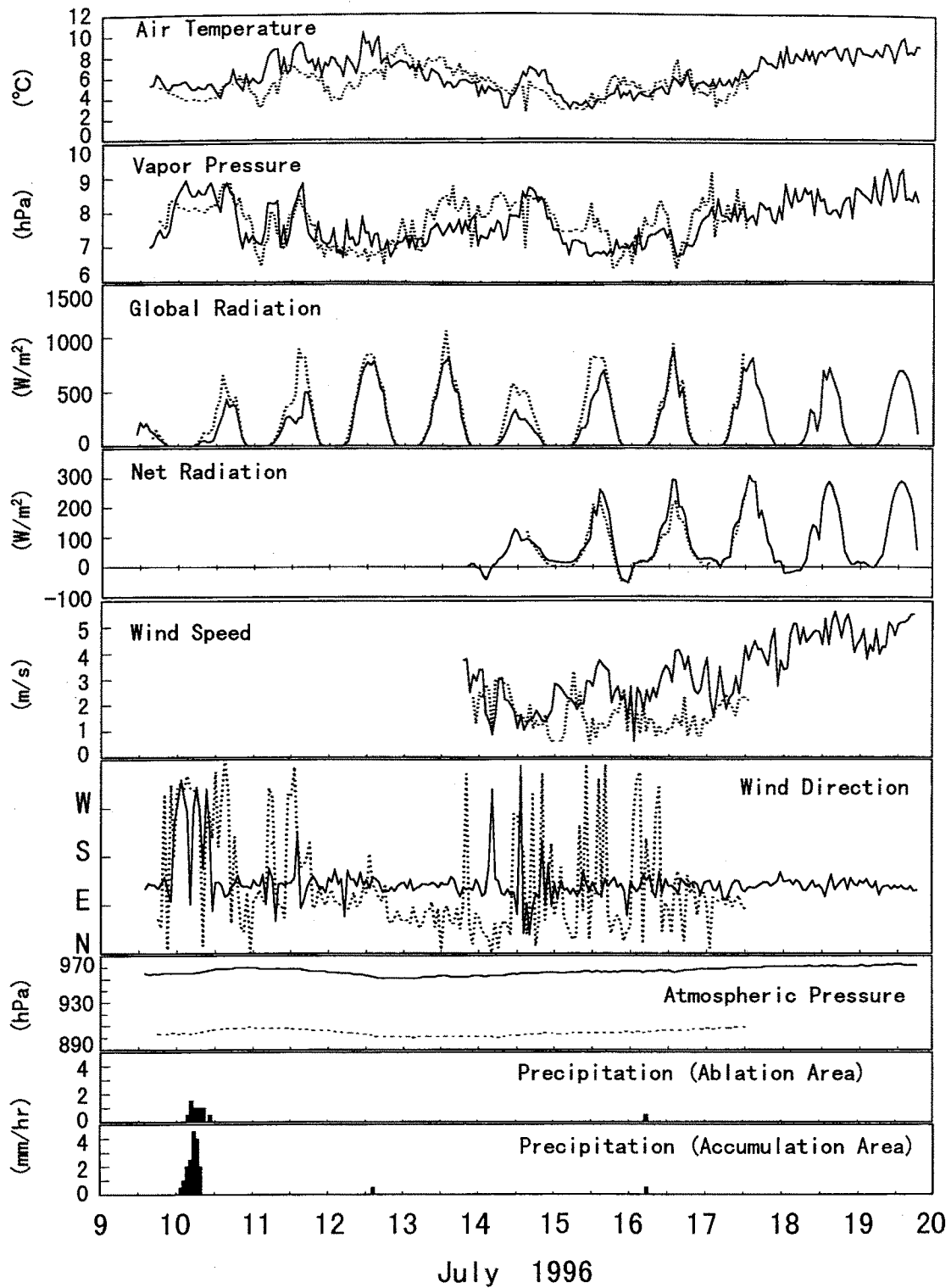


Fig. 2 Meteorological components observed at the ablation station (solid line) and accumulation station (dotted line).

ture of the accumulation station is higher than that of the ablation station. This could be thought that air temperature at the accumulation station was raised under the Foehn type phenomena, in which air raised on the out side slope of the glacier ridge, forming precipitating cloud, become dryer and came down adiabatically on the inner side of the glacier ridge raising the temperature.

Vapor pressure at the two stations is always higher than that of saturation vapor pressure of ice at 0 °C. This means that vapor in the air was sublimating (condensation) to the glacier surface all the time, giving the latent heat of sublimation for melting. The range of the vapor pressure variation is from 6.5 hPa to 9 hPa. Similar to the air temperature variation, the diurnal variation of vapor pressure is not clear for the both station and the difference of the two station in vapor pressure suggests that the vapor pressure of air parcel at the accumulation station was not conserved when it reached to the ablation station or the air masses at the two station is not the same.

4.1.2 Global and net radiation

Global radiation at the accumulation station was larger than that at the ablation station almost all the observation period. When it is cloudy at the ablation station (smaller global radiation), the global radiation at the accumulation station was much larger than that of ablation station. This is explained that, when it is cloudy, the ablation station is under the cloud and the accumulation station is in the cloud. The global radiation reaching to the accumulation station is less disturbed by the cloud due to the thinner layer of the cloud.

The daily sum of the global radiation of the accumulation station is almost larger than that of the ablation station, whereas that of net radiation is not. This is mainly due to the difference in albedo of the surface and atmospheric radiation. The albedo at the accumulation station is 0.66 and at the ablation station 0.62. The smaller global radiation at the ablation station indicates the larger cloudiness, which reveals the larger atmospheric radiation.

4.1.3 Wind speed and direction

The prevailing wind direction at the ablation station is southeasterly, which is the same as the glacier flow direction there and more constant than that at the accumulation station.

The wind speed at the ablation station was much

larger than that at the accumulation station. This is because the ablation station is located in the downstream of the glacier, therefore, katabatic wind, which is a cooled air drainage, was more developed at the ablation station, and that the ridge-to-ridge distance laterally to the glacier flow direction is smaller at the ablation station than that at the accumulation station, therefore, the air flow is received so called "funnel effect." (Parish and Bromwich, 1986).

4.1.4 Atmospheric pressure and precipitation

The atmospheric pressure at the two stations showed same trend. It increased by the late night of July 10, decreased till the night of July 12, and then increased gradually by the end of the observation.

The atmospheric pressure difference of the two stations was 51.5 hPa. From the hydrostatic equation and the ideal gas law, assuming no horizontal pressure gradient between the accumulation station and a point at the height of the accumulation station above the ablation station, the average temperature of the layer between the two station can be expressed as (see Appendix):

$$T_{pres} = (g/R) \cdot ((z_1 - z_2) / \ln(P_2/P_1)) \quad (1)$$

where T_{pres} is the average temperature of the layer between the two station, g the gravitational acceleration, R the dry gas constant, z the elevation and P the atmospheric pressure. Suffix 1 and 2 denotes the lower and upper station, respectively. The average T_{pres} in the observation period was calculated as 9.6 °C. Since the average temperature for the two station is 5.6 °C, the difference of 4.0 °C could be due to the cooling by the glacier surface and/or the horizontal pressure difference (it was assumed to be 0).

There was a rainfall event in the morning of July 10 and 16 for the both stations. It was 16.5 mm at the ablation station and 5.5 at the accumulation station on July 10, and 0.5 mm for the both station on July 16. The 0.5 mm of rainfall in the afternoon of July 12 was only recorded at the ablation station.

4.2 Observed hydrological elements

The measured hydrological data are shown in Fig. 3. They are measured at 100 m downstream from the terminus of the glacier on the Stream A. The flow amount of Stream B was manually measured and it was less than 20 % of that in Stream A. The source of water in Stream B was mainly the meltwater of the seasonal snow accumulated on the

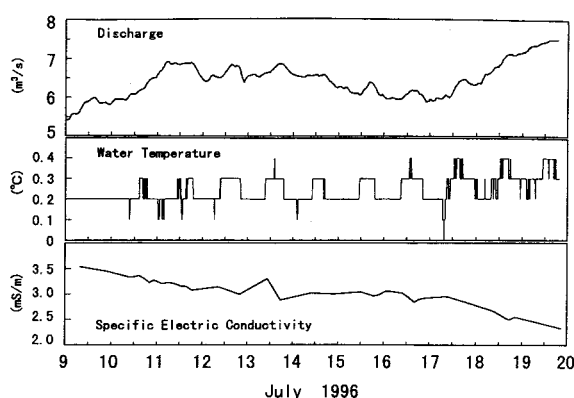


Fig. 3 Hydrological terms observed at the Stream A.

steep side slope of the glacier. Therefore, Stream B was disregarded in this study.

4.2.1 Discharge

Water level of the Stream A was recorded to a data logger every 10 minutes. The cross-sectional area and flow rate was measured manually 7 times. The Q-L curve was obtained relating the water level and discharge rate. Then the discharge rate was calculated using the relationship from the water level and the 2 hour running mean was taken (top figure in Fig. 3).

The discharge of Stream A increased gradually from $5.5 \text{ m}^3/\text{s}$ to $7.5 \text{ m}^3/\text{s}$. The daily maximum discharge occurred around 1400 to 1800 in Kamchatka Standard Time (KST), but diurnal cycle is faintly seen.

The line connecting the daily minimum discharge rate (base flow, not shown) increased till July 14, decreased afterward till July 16, and increased towards the end of observation period. Diurnal variation of the discharge rate was obvious except on July 10, when the rainfall was recorded. The daily sum of discharge amount larger than the base flow (the line connecting the daily minimum discharge rate) well corresponds to the daily global radiation, which is the main heat source for snowmelt.

4.2.2 Water temperature

The stream temperature is shown in the second figure in Fig. 3. Since the resolution of the thermometer is $0.1 \text{ }^\circ\text{C}$, the temperature changes like stairs. The stream temperature was about $0.2 \text{ }^\circ\text{C}$ almost all the time until July 17, and then about $0.1 \text{ }^\circ\text{C}$ increased towards the end of observation. This increase of

temperature might be due to the increase of uncovered area by snow over the stream. A block of ice and snow was sometimes floating in the stream, which might make the water temperature fluctuate.

4.2.3 Specific electric conductivity (SEC)

The SEC of Stream A was gradually decreasing in the observation, although sometimes a small fluctuation was observed. The relationship of SEC with the discharge rate is discussed in the next chapter.

5. Discussion

5.1 Heat balance

Heat balance of the glacier surface is expressed as follows :

$$M = R + S + L \quad (2)$$

where M is the heat used for snowmelt, R the net radiation, S the sensible heat flux and L the latent heat flux. Since the surface temperature was all the time $0 \text{ }^\circ\text{C}$ and the temperature profile near surface in the snow/firn was also $0 \text{ }^\circ\text{C}$ (Shiraiwa *et al.* 1997), conductive heat flux in snow/ice was assumed to be negligible. The heat used for snowmelt was obtained from the surface lowering measured using snow stakes and surface snow density. The net radiation was measured as shown in the Fig. 2. The sensible and latent heat fluxes are calculated using so called "bulk method." using following equations :

$$S = A \cdot V \cdot (T_a - T_0), \quad (3)$$

$$L = B \cdot V \cdot (e_a - e_0). \quad (4)$$

where V is the wind speed (m/s), T_a the air temperature ($^\circ\text{C}$), T_0 the surface temperature, e_a the vapor pressure of air (hPa), and e_0 (hPa) the saturated vapor pressure of the surface, which temperature is $0 \text{ }^\circ\text{C}$. The coefficient A and B was tuned to best fit to the following equation by trial and error,

$$A \cdot V \cdot (T_a - T_0) + B \cdot V \cdot (e_a - e_0) = M - R. \quad (5)$$

At the accumulation station, the bulk coefficient A was $7.0 \text{ J}/(\text{m}^3 \cdot \text{ }^\circ\text{C})$ and B was $19.3 \text{ J}/(\text{m}^3 \cdot \text{ hPa})$. For the ablation station A and B are 3.0 and 7.5, respectively. From these values, the bulk transfer coefficient at the accumulation station are obtained as 5.5×10^{-3} and 8.8×10^{-3} for the sensible and latent heat fluxes, respectively. For the ablation station they are 2.3×10^{-3} and 3.8×10^{-3} . A bulk transfer coefficient is

depending on the roughness and turbulent intensity as well as the heights of the temperature, humidity and wind speed measured. The different values obtained here was due to the combination of these variables and the accuracy of snowmelt intensity measurement.

The results of the heat balance calculation is summarized Fig. 4 and Table 2. The largest heat source for the glacier ablation was the net radiation, which is, as an average, about 45 % of the total heat used for melting. The second largest is the sensible heat flux and the third is the latent heat flux, which are about 30 % and 25 % of the snowmelt heat,

respectively. When the large daily snowmelt occurs, the largest heat source for snowmelt is not the net radiation but the sensible heat flux (e.g. for the case of July 18 at the ablation station). The larger the daily snowmelt intensity was, the larger the turbulent (sensible and latent) heat fluxes were.

The ratio of the components for snowmelt heat balance of Koryto glacier was compared with those for seasonal snow in Spitsbergen, Moshiri Experimental Forest, Hokkaido, Japan and Hisago snowpatch, Hokkaido, Japan (Fig. 5). The net radiation is the largest heat source for the snowmelt for all those

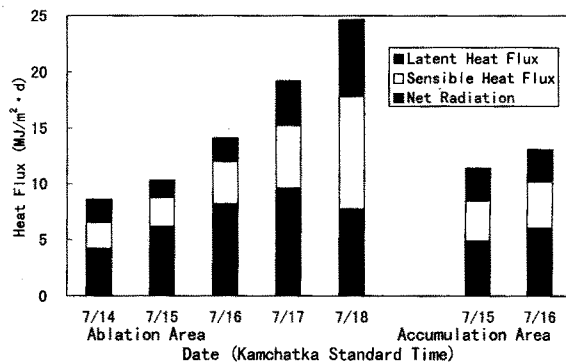


Fig. 4 Results of heat balance calculations.

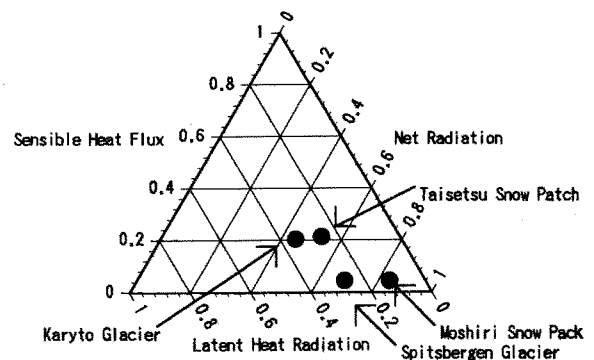


Fig. 5 Triangle diagram of the ratios for the net radiation, Sensible heat flux and latent heat flux to the total heat used for snowmelting for Koryto glacier, seasonal snow in Spitsbergen, Moshiri Experimental Forest, Hokkaido, Japan and Hisago snowpatch, Hokkaido, Japan.

Table 2 Heat balance component and its ratio of Koryto Glacier

Heat balance components			
Date	Net Rad.	Sens. Heat Flux	Latent Heat Flux
	(MJ/m ² ·d)	(MJ/m ² ·d)	(MJ/m ² ·d)
Ablation Station			
Jul. 14	4.18	2.36	2.07
Jul. 15	6.16	2.60	1.54
Jul. 16	8.18	3.81	2.12
Jul. 17	9.61	5.64	3.99
Jul. 18	7.73	10.11	6.83
Accumulation Station			
Jul. 15	4.89	3.57	2.93
Jul. 16	6.02	4.17	2.91
Ratio to the heat used for snowmelt			
Ablation Station			
	(%)	(%)	(%)
Jul. 14	48.5	27.5	24.0
Jul. 15	59.8	25.3	14.9
Jul. 16	58.0	27.0	15.0
Jul. 17	49.9	29.3	20.8
Jul. 18	31.3	41.0	27.7
Accumulation Station			
Jul. 15	42.9	31.4	25.7
Jul. 16	46.0	31.8	22.2

places. For the Koryto glacier the ratio of the net radiation is the smallest among those places. This is due to the larger wind speed, which makes the larger turbulent fluxes. Unfortunately, the data in Koryto glacier is very short comparing to the other sites mentioned above. Therefore, it is not appropriate to say that above results are true for the whole melting period. However, as revealed from the discharge-electric conductivity relationship in the following paragraph, what mentioned above would be true at least for the early stage of the melting season.

5.2 Runoff

Fig. 6 shows the mean diurnal variation of the discharge rate of the Stream A (solid line) for the whole observation period. The dotted line shows the mean value plus the standard deviation and the broken dotted line shows the mean value minus the standard deviation. Since the discharge rate at the hour 24 is larger than that at the hour 00, the discharge is increasing in this period. This means that the ablation is in its beginning stage and as Fountain (1996) says, the slowly varying component of the discharge can be explained by the volume of daily meltwater input into the accumulation area. The diurnal range of the mean discharge rate is about $0.3 \text{ m}^3/\text{s}$, which is smaller than the mean value of standard deviation of about $0.35 \text{ m}^3/\text{s}$. This indicates that the daily discharge pattern is not so consistent.

Arrows in Fig. 6 indicates the time of maximum

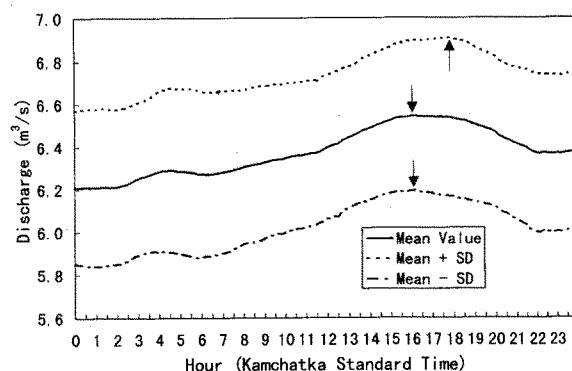


Fig. 6 Mean diurnal discharge rate (solid line) and curves for the standard deviation added (dotted line) and subtracted (broken-dotted line). The arrows indicate the time of the maximum value occurred.

discharge rate occurred. The maximum of mean discharge rate occurred at 1600 KST. Since the solar noon at this place is about 1300 KST and the peak melting could occur at the solar noon, the lag time from peak melting rate to the peak discharge rate can be estimated to be about 3 hours. The curve for the mean value minus the standard deviation showed the almost same peak time of day but the curve for the mean value plus the standard deviation showed 2 hours of delay in peak time from the mean curve. This means that the larger discharge rate indicates the larger contribution of the further area (accumulation area), which takes more time to reach to the terminus of the glacier. This is consistent with the explanation obtained for the slowly varying discharge component of the discharge mentioned above.

Fig. 7 shows that the relationship between the discharge rate and the specific electric conductivity (SEC). As an average, the SEC is decreasing with the increase of the discharge rate. This can be generally explained as "diluting effect" of meltwater and it occurs at the beginning of the ablation period (Kodama *et al.* 1995). There are 3 stages in the relationship in the figure: first is the first diluting period until July 14 (see also Fig. 3); second is the period SEC was unchanged or a little increasing with the discharge rate decreasing; third is the second diluting period. This hysteresis nature of the relationship is very interesting but we do not have a clear explanation.

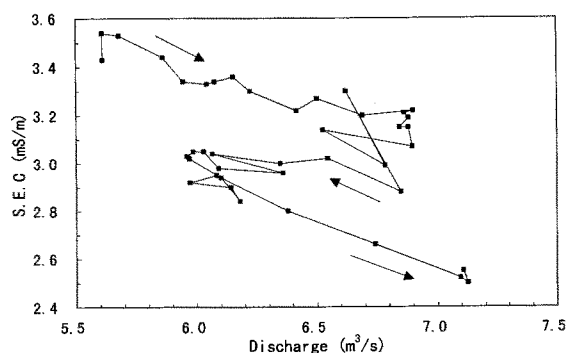


Fig. 7 Relationship of Specific electric conductivity to Discharge rate. The arrows indicate the time sequence.

6. Summary

Meteorological observations were carried out at ablation and accumulation stations of the Koryto glacier, Kamchatka, in order to understand the characteristics of melting heat balance components. The results of the heat balance calculation showed that the largest heat source for the glacier ablation is the net radiation, which is, as an average, about 45 % of the total heat used for the melting. The second largest is the sensible heat flux and the third is the latent heat flux, which are about 30 % and 25 % of the snowmelt heat, respectively. When the large daily snowmelt occurs, the largest heat source for the snowmelt is sometimes not the net radiation but the turbulent heat fluxes.

Hydrological observations were carried out at two runoff streams from Koryto glacier. In Stream A, which had more than 5 times larger discharge than that of Stream B, water level, water temperature and specific electric conductivity were recorded. The discharge of Stream A increased gradually from 5.5 m³/s to 7.5 m³/s. The daily maximum discharge occurred about 3 hours later than the solar noon and the time lag was increased when the discharge became larger. The relationship between the specific electric conductivity and the discharge rate showed that the dilution of englacial constituent and/or stream bed material was progressing. Those hydrological results indicates that the ablation is in its beginning stage.

Acknowledgments

We would like to express our sincere thanks to Mr. Sveltslav Bogotov and Mr. Igor Markov for their logistical support in the field camp. We are also indebted to the staffs of the machine shop of ILTS for their support making or modifying the equipment used in the field. This study was supported by a Grant-in-Aid for International Scientific Research (No. 0841090 : Principal Investigator D. Kobayashi) of the Ministry of Education, Science, Sports and Culture of Japan.

References

1. Fountain, A.G. (1996) : Effect of snow and firn hydrology on the physical and chemical characteristics of glacial runoff. *Hydrol. Processes*, **10**, 509–521.
2. Kodama, Y., Takeuchi, Y., Nakabayashi, H. and Watanabe, O. (1995) : Hydrological observations in Bregger Glacier basin, Spitsbergen-discharge, temperature and electric conductivity-. *Proc. NIPR Sympo. Polar Meteorol. Glaciol.*, **9**, 45–53.
3. Parish, T.R. and Bromwich, D.H. (1986) : The inversion wind pattern over West Antarctica. *Mon. Wea. Rev.*, **114**, 849–860.
4. Shiraiwa, T., Muravyev, Y., Yamaguchi, S., Glazirin, G.E., Kodama, Y. and Matsumoto, T. (1997) : Glaciological features of Koryto Glacier in the Kronotsky Peninsula, Kamchatka, Russia. *Bull. Glacier Res.*, **15**, 27–36.

Appendix

If a layer is in the hydrostatic equilibrium, the pressure difference, dP , between the top and bottom of the layer and the thickness, dz , of the layer can be expressed :

$$dP = -\rho g dz. \quad (A-1)$$

where ρ is the air density and g the gravitational acceleration. The ideal gas law can be expressed :

$$P = \rho R T \quad (A-2)$$

where P is the atmospheric pressure, R the ideal gas constant and T the air temperature. When (A-2) puts into (A-1), it becomes :

$$dP = -(P/R T) g dz. \quad (A-3)$$

Assuming the temperature of the layer is isothermal (T_{pres}), integration of (A-3) becomes :

$$\ln(P_2/P_1) = -(g/R T_{pres}) (z_2 - z_1). \quad (A-4)$$

Putting the T_{pres} to the left hand side of the equation, (A-4) becomes :

$$T_{pres} = (g/R) ((z_1 - z_2)/\ln(P_2/P_1)) \quad (A-5)$$

The equation (A-5) means that, if the atmospheric pressures at the two heights are known, the average air temperature can be calculated. If the dry gas constant is used, T_{pres} is an apparent temperature.